Jurnal Riset Kimia

ISSN (print) : 1978-628X
ISSN (online) : 2476-8960

Synthesis of Pyridazinone Derivatives Substituted with Methoxy with Phenyl Hydrazine and In Silico Test of Anticancer Activity

Winda Permata[1], Putri Mar[1], Hilwan Yuda[1] , and Jasril[1*]

[1]Department of Chemistry, Faculty of Mathematics and Natural Sciences (FMIPA), Riau University, Pekanbaru, Indonesia

Corresponding Author:
Jasril
jasril.k@lecturer.unri.ac.id

Received: December2024
Accepted: August 2025
Published: September 2025

Abstract

The synthesis of pyridazinone derivatives has gained increasing attention due to their diverse biological activities, particularly as anticancer agents. In this study, novel pyridazinone derivatives substituted with methoxy groups and phenyl hydrazine were synthesized through a multi-step reaction pathway, starting from methoxyacetophenone and glyoxylic acid, followed by cyclization and substitution reactions to yield the target compound 7-(2-methoxyphenyl)-2H-pyridazino[6,1-c][1,2,4]triazine-3(4H)-one. The synthesized compounds were characterized by melting point, TLC, HPLC, UV-Vis, FTIR, NMR, and MS analyses, confirming the expected structures. In silico evaluation was performed using molecular docking against estrogen receptor α (ERα) kinase domain (PDB ID: 1T46), a key protein in breast cancer progression. The docking results showed that the synthesized compounds exhibited strong binding affinities, with compound 8 displaying a binding free energy of –9.1971 kcal/mol and stable interactions with residues Cys673, Leu799, and Phe811. These values were superior compared to the natural ligand and comparable to the reference drug doxorubicin, indicating significant anticancer potential. The results suggest that structural modification of pyridazinone with methoxy and phenyl hydrazine substituents enhances its cytotoxic activity, making it a promising candidate for further development as an anticancer agent.

Keywords: *Pyridazinone, phenyl hydrazine, in silico, breast cancer, estrogen receptor α.*

Introduction

The synthesis of drug compounds is an important step in the development of therapies for various diseases, including cancer. In recent years, considerable attention has been given to heterocyclic compounds, particularly pyridazinones, which show potential as anticancer agents [1]. The nitrogen-rich structure of pyridazinones contributes to their broad biological activity [2]. Analogues of pyridazinone derivatives are used in the treatment of various human pathological conditions [3]. Pyridazinone has been reported to possess anticonvulsant activity [4], analgesic, anti-inflammatory, and antimicrobial activity [5], antihypertensive activity [6], as well as anticancer activity. This diversity of biological activities makes it an attractive candidate in the search for new drugs. Substitutions on the pyridazinone core ring can influence its efficacy and specificity toward specific biological targets [7].

Pyridazinones and their derivatives have been shown to have the ability to inhibit cancer cell growth, making them attractive candidates for cancer therapy. The chemical structure of pyridazinones, which is rich in nitrogen atoms, gives them unique chemical properties that allow these compounds to interact with various biological targets involved in cancer development. Previous studies have shown that pyridazinone can modulate signaling pathways involved in cell proliferation, which is key to the formation and development of tumours [8].

Furthermore, research shows that structural modifications to pyridazinone compounds, such as the addition of a methoxy group to the phenyl ring, can significantly increase cytotoxic activity against cancer cells. This methoxy group can increase the solubility of the compound in organic solvents and improve interactions with biological targets, thereby enhancing the therapeutic potential of the compound [9]. Additionally, other substitutions on the pyridazinone ring, such as the addition of phenyl hydrazine, offer additional potential in enhancing anticancer activity by strengthening the compound's interactions with target molecules in cancer cells.

Cancer is one of the leading causes of death worldwide, with prevalence continuing to rise, particularly in developing countries. In Indonesia, breast and cervical cancer are the most common types of cancer among women, resulting in high mortality rates [10]. This increase in incidence highlights the urgent need for the development of more effective and safer therapies. One promising approach in cancer treatment is the synthesis of heterocyclic compounds, particularly pyridazinones, which have potential as anticancer agents. The nitrogen-rich chemical structure of pyridazinones allows these compounds to interact with various biological targets and modulate cellular signalling pathways involved in cancer cell proliferation.

At the molecular level, one of the most relevant biological targets in the development of breast cancer therapies is the 1T46 protein, which is a crystal domain of the estrogen receptor α (ERα) DNA-binding domain. This protein plays a crucial role in the development and growth of breast cancer cells influenced by estrogen. The crystal structure of 1T46 provides important insights into how the interaction between estrogen and ERα affects cancer cell proliferation [8]. Therefore, inhibiting this interaction is a potential therapeutic strategy in breast cancer treatment.

One important aspect in the development of breast cancer is the role of tyrosine kinase in the process of cell proliferation. Tyrosine kinase, whether in the form of receptor tyrosine kinase (RTK) or non-receptor tyrosine kinase (NRTK), is involved in signal transduction that regulates cell growth and the survival of cancer cells. When tyrosine kinases are activated either through interaction with ligands or mutations causing constitutive activation, tyrosine phosphorylation of target proteins activates signalling pathways involved in cancer cell proliferation, invasion, and metastasis. In the context of breast cancer, several tyrosine kinase receptors, such as EGFR and HER2, are often overexpressed or mutated, contributing to tumour development [11].

Inhibition of tyrosine kinase can slow down the growth of cancer cells by disrupting the signalling pathways required for cell proliferation. Anticancer compounds that can inhibit tyrosine kinase activity, such as those found in some tyrosine kinase inhibitors (TKIs), have shown great therapeutic potential. Structurally modified pyridazinone derivatives are expected to enhance their interaction with tyrosine kinase receptors or target proteins, thereby increasing their efficacy as more selective anticancer agents with a lower toxicity profile compared to conventional chemotherapy agents such as doxorubicin [12].

Based on the above description, this study conducted the synthesis of pyridazinone derivatives and in silico anticancer activity testing (molecular docking) against tyrosine kinase protein receptors. The synthesized pyridazinone compounds were designed to have methoxy and phenyl hydrazine substituents coordinated with nitrogen atoms in the pyridazinone framework. The nitrogen atoms in the target compound have electronegative properties and can form hydrogen bonds, which have the potential to inhibit tyrosine kinase activity. The biological activity of the synthesised pyridazinone was tested as an anticancer agent in silico against the tyrosine kinase receptor (PDB ID: 1T46).

DOI: https://doi.org/10.25077/jrk.v16i2.809

Experimental

Equipment

The equipment used in this study included an analytical balance (NEWTECH), magnetic stirrer, ACE pressure tube, KLT vessel, hotplate (BOECO Germany), oven, Fisher John melting point apparatus (SMP 11-Stuart), UV lamp (Camag® 254 and 365 nm), UV -Vis (Genesys 10 UV-VIS v4.002219N175013), HPLC (UFLC Prominance Shimadzu LC Solution, UV SPD 20AD detector, C18 column (ODS, Octadecylsilane)), FTIR spectrophotometer (FTIR Shimadzu, IR Prestige-21), NMR spectrophotometer (Agilent 500 MHz with DD2 console system), mass spectrophotometer (Water LCT premier XE positive mode), and common glassware used in the Chemistry Laboratory of the Faculty of Mathematics and Natural Sciences, University of Riau.

Material

The chemicals used in this study included *2-methoxyacetophenone*, *3,4-dimethoxyacetophenone*, *glyoxylic acid*, *hydrazine monohydrate*, *glacial acetic acid*, *ethyl chloroacetate*, *phenylhydrazine*, *potassium carbonate*, *ethanol*, *methanol*, *ethyl acetate*, *sodium hydroxide*, *dimethylformamide*, and *n-hexane*, which were purchased from PT. Multi Medika Laboratory.

Methods

Synthesis 6-(2-metoksifenil)piridazin-3(2H)-on (4)

2-methoxyacetophenone (1) (0.598 g; 3 mmol), *glyoxylic acid* (2) (0.276 g; 3 mmol) and *glacial acetic acid* (3 mL) were mixed into an ACE pressure tube. The mixture was reacted at 120°C for 4 hours while stirring using a magnetic stirrer. Reaction monitoring was performed every hour using thin-layer chromatography (TLC). Subsequently, after the formation of the intermediate compound, *monohydrate hydrazine* (0.15 g; 3 mmol) was added to the mixture, and the reaction was continued under the same conditions for 3 hours. Reaction monitoring is performed every hour using TLC. After the reaction is complete, the mixture is added with cold DM water and neutralised using 6N NaOH. The pH of the mixture is measured using a universal indicator. The mixture is then placed in a freezer and left for 24 hours to form a precipitate. The resulting solid was filtered using Whatman filter paper, rinsed with cold n-hexane, and dried at room temperature. The impure pyridazinone solid was then recrystallised using an appropriate solvent. The obtained solid was tested for purity using TLC, melting point measurement, and HPLC analysis.

Synthesis of ethyl-2-(3-(2-methoxyphenyl)-6-oxopyridazin-1(6H)-yl)acetate (6)

The compound *6-(2-methoxyphenyl)pyridazin-3(2H)-one* (4) (0.252 g; 1 mmol), *ethyl chloroacetate* (5) (0.184 g; 1.5 mmol), and *potassium carbonate* (0.276 g; 2 mmol) were mixed in an Erlenmeyer flask. Five millilitres of dimethylformamide solvent were added to the Erlenmeyer flask, and the mixture was stirred for 3 hours at room temperature. The reaction process was monitored using thin-layer chromatography (TLC). After the reaction was complete, the mixture was poured into a container containing ice and DM water, then stored in a freezer for 24 hours until a precipitate formed. The resulting solid is filtered using Whatman filter paper and dried at room temperature. The purity of the solid is then analysed through TLC testing, melting point determination, and analysis using HPLC.

Synthesis of the compound 7-(2-methoxyphenyl)-2H-pyridazino[6,1-c][1,2,4]triazine-3(4H)-one (8)

Ethyl-2-(3-(2-methoxyphenyl)-6-oxopyridazin-1(6H)-yl)acetate (6) (0.288 g; 1 mmol) was dissolved in 25 mL of *methanol* in an Erlenmeyer flask. 3 mL of *phenyl hydrazine* (7) and *NaOH* were added to the reaction mixture, then stirred for 3 hours at 80 °C. The reaction progress was monitored using thin-layer chromatography (TLC). After completion, the precipitate formed was filtered and washed with n-hexane. The remaining n-hexane solvent is discarded, and the solid is dried at room temperature. The obtained solid is then tested for purity via TLC, melting point determination, analysed using HPLC, and structural confirmation.

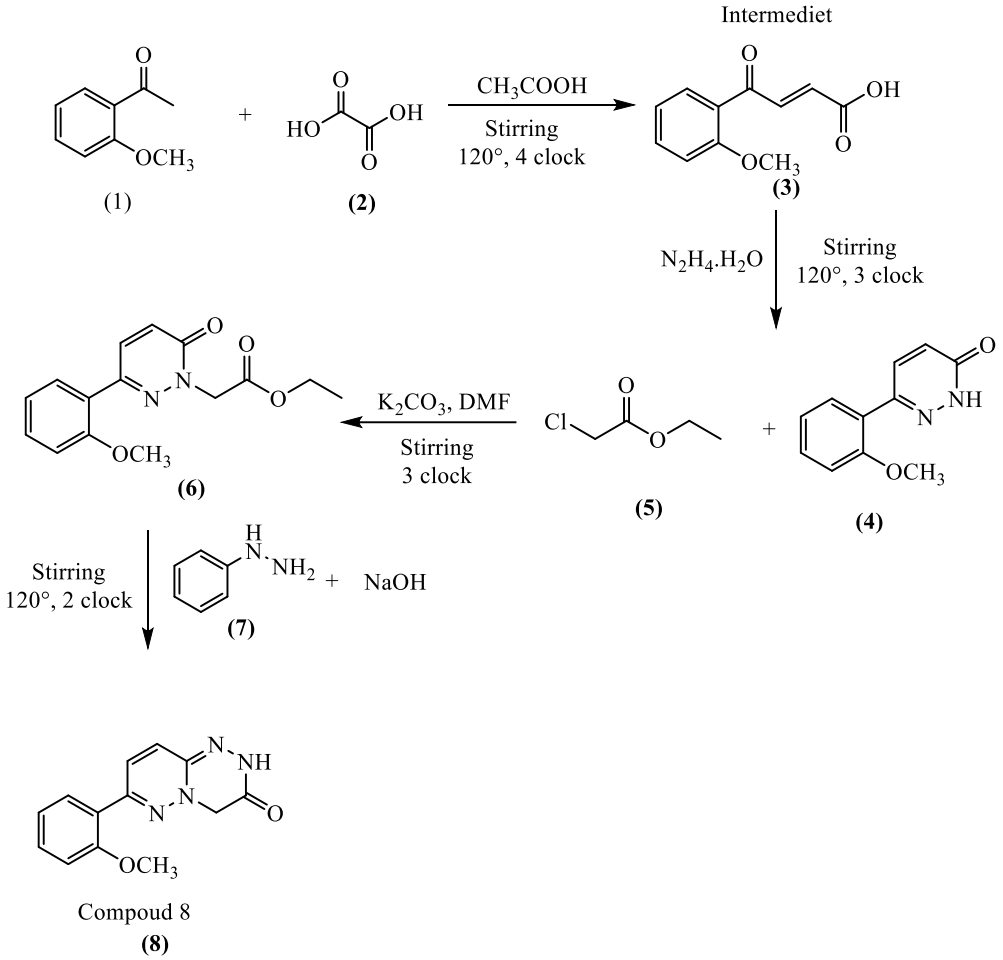

Figure 1. Mechanism of synthesis of pyridazinone derivatives

Molecular Docking Simulation

Open the MOE program by double-clicking on the icon on the desktop. Next, open the prepared protein file by clicking File→ Open→ select file 1T46 Prep 2→ OK→ Yes. The active site of the protein is then determined by running the command Compute→ Site Finder→Apply→ select Site 1→ Dummies→Yes. Next, return to the main page, select the Compute menu → Dock → Density → select the file logo on the right, then select the ligand file in .mdb format. Ensure that the selected ligand file is correct. Next, change London dG to 100 and Refinement to 10. Save the docking file in .mdb format, then click Run and wait until the docking process is complete.

After the docking process is complete, a table will appear in the docking results database. Next, select the File menu in the docking results database and click Browse. Select the ligand position that meets the RMSD < 2 requirement. To view the interaction between the ligand and receptor after docking, select the Compute menu → Ligand Interactions →then the visualisation of the ligand interaction with the amino acid residue will be displayed.

Measurement

Compound 4

Compound 4: Molecular formula *C11H10N2O2*, a yellowish-brown solid with a yield of 92.4%, melting point 164–166°C. Rf values for the compound were obtained as 0.47 (n-hexane : ethyl acetate 6 : 4), 0.68 (chloroform : ethyl acetate 6 : 4), and 0.8 (methanol : ethyl acetate 6 : 4). HPLC (λ = 254 and 365 nm) tR 6.32 minutes. UV spectrum (MeOH) λmax = 250 nm. FTIR spectrum (KBr): ῡ (cm−1): 3416 (N-H), 3069

DOI: https://doi.org/10.25077/jrk.v16i2.809

(aromatic C-H), 2992 (aliphatic C-H), 2840 (-CH2-), 1686 (C=O), 1593 (C=C), 1265 (C-O), 1223 (C-N).

Compound 6

Compound 6: Molecular formula *C14H14N2O4*, a yellow solid with a yield of 96.8%, melting point 98°C. Rf values of the compounds obtained include 0.8 (n-hexane : ethyl acetate 4 : 6), 0.8 (chloroform : ethyl acetate 6 : 4), and 0.8 (dichloromethane : ethyl acetate 6 : 4). HPLC (λ = 254 and 365 nm) tR 4.78 minutes. UV spectrum (MeOH) λmax = 249 nm. FTIR spectrum (KBr): $\bar{\upsilon}$ (cm−1): 3042 (aromatic C-H), 2939 (aliphatic C-H), 2842 (-CH2-), 1739 (ester C=O), 1673 (C=O), 1592 (C=N), 1309 (C-O), 1222 (C-N).

Compound 8

Compound 8: Molecular formula *C13H12N4O2*, a yellow solid with a yield of 85.8%, melting point ±200°C. The Rf values of the compound were obtained as 0.53 (methanol : ethyl acetate 4 : 6), 0.8 (methanol : chloroform 7 : 3), and 0.8 (methanol : dichloromethane). HPLC (λ = 215 and 254 nm) tR 3.53 minutes. UV spectrum (MeOH) λmax = 249 nm. FTIR spectrum (KBr): $\bar{\upsilon}$ (cm^(−1)): 3500 (N-H), 3056 (aromatic C-H), 2937 (aliphatic C-H), 2842 (-CH_2—), 1667 (C=O), 1650 (C=N), 1307 (C-O), 1243 (C-N). MS (m/z) calculated as C19H20N4O2 [M+H]+: 336.39 and found at (m/z) $[M+H]^+$: 33.0187.

^{1}H-NMR (MEOD-Bruker, 500 MHz): δ 7.85 (dd, J=1.6 Hz, 1H, H-3'); 7.61 (d, J=7.6 Hz, 1H, H-5); 7.44 (t, J=7.3 Hz, 1H, H-5'); 7.12 (dd, J=1.8 Hz, 1H, H-4); 7.05 (t, J=7.7 Hz, 1H, H-4'); 6.95 (dd, J=1.65 Hz, 1H, H-6'); 4.79 (s, 2H, H-1''); 3.88 (d, J=1.1 Hz, 3H).

^{13}C-NMR (MEOD-Bruker, 125 MHz) δ = 54.7 (-CH3); 55.8 (-CH2-); 111.2 (-CH-); 120.5 (-CH-); 124.3 (C=C); 127.3 (-CH-); 130.0 (-CH-); 130.7 (-CH-); 135.1 (-CH-); 145.3 (C-O); 157.2 (C=N); 160.8 (C=N); 172.9 (C=O).

Results and Disscusion

Synthesis of compound 4

Compound 4 was synthesised through a one-pot condensation reaction of *acetophenone* with *glyoxylic acid* in an acidic environment, which was then cyclised using *hydrazine hydrate* to form a pyridazinone ring. The one-pot method was chosen because it is simple, efficient, and environmentally friendly. *Glacial acetic acid* acted as a catalyst, enabling the formation of an enol ion intermediate. The protonation of the carbonyl oxygen in the ketone compound makes it more electrophilic, facilitating the formation of a stable carbocation through resonance. The C=C double bond formed during this process accelerates the subsequent steps, namely deprotonation and dehydration, resulting in an α,β-unsaturated compound, which is then followed by a cyclisation reaction to form pyridazinone [13]. This mechanism demonstrates that the acid catalyst not only aids in the formation of the enol ion but also plays a role in the dehydration essential for the formation of the pyridazinone structure. The reaction mechanism for the formation of oxobutenoic acid compounds is shown in Figure 2.

The synthesis of pyridazinone compounds occurs through a cyclisation reaction mechanism, in which hydrazine hydrate acts as a nucleophile that attacks the carbonyl carbon in oxobutenoic acid, forming a pyridazinone ring. This reaction requires the assistance of H+ and OH− ions to facilitate the formation of the final product [14]. This cyclisation process leads to the formation of a heterocyclic structure with two nitrogen atoms, which are important for enhancing the biological activity of pyridazinone compounds. The reaction mechanism for the formation of pyridazinone compounds is shown in Figure 3.

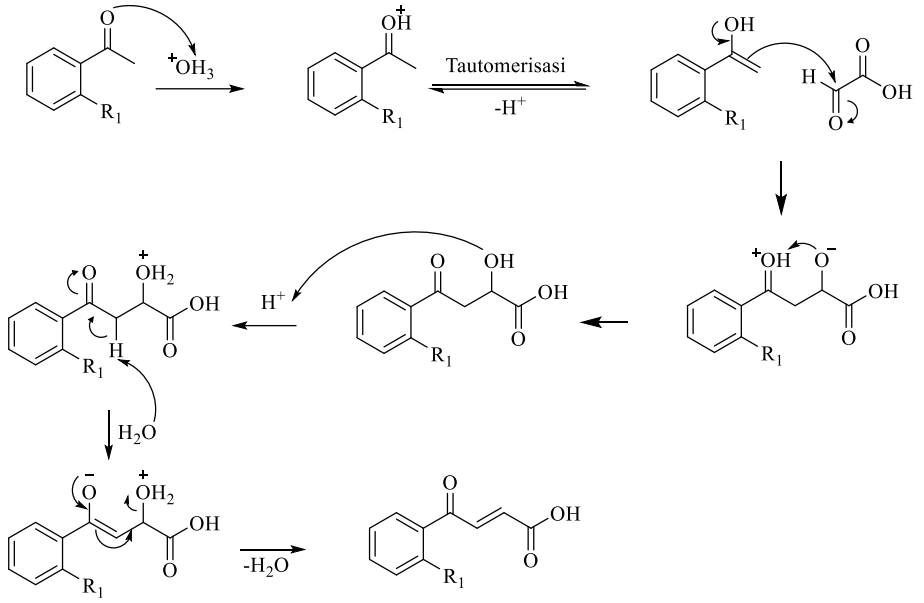

Figure 2. Reaction mechanism for the formation of oxobutenoic acid compounds

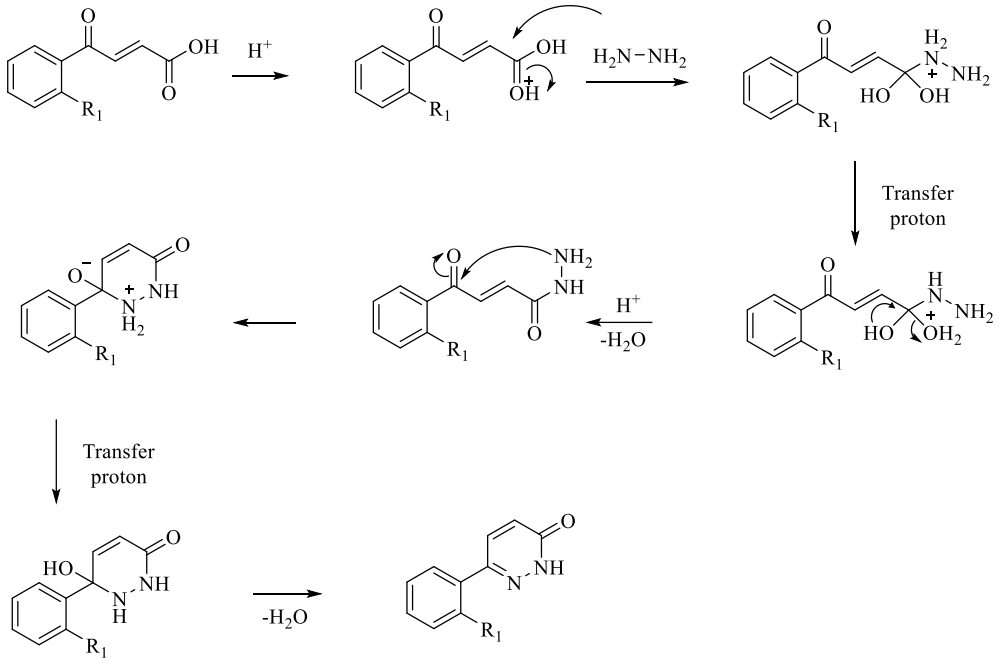

Figure 3. Reaction mechanism for the formation of compound 4

The process was monitored with TLC until the reaction was complete in 8 hours, then the product was precipitated, filtered, and washed with cold solvent to purify the result. Compound 4 was obtained as a brownish-yellow solid with a yield of 92.4% (Figure 4).

Characterisation was performed using TLC, HPLC, melting point, and FTIR. The HPLC results showed one dominant peak at wavelengths of 254 nm and 365 nm, indicating high purity. The FTIR spectrum showed characteristic absorptions of pyridazinone, including: N–H (3416 cm^{-1}), C=O (1686 cm^{-1}), aromatic C=C (1593 cm^{-1}), and methoxy C–O (1265 cm^{-1}). These data support the formation of the expected methoxy-substituted pyridazinone structure.

DOI: https://doi.org/10.25077/jrk.v16i2.809

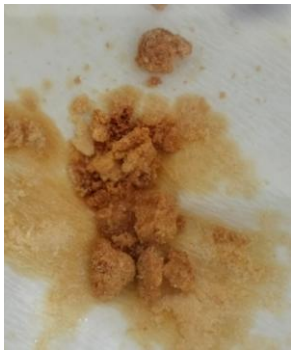

Figure 4. Compound product 4

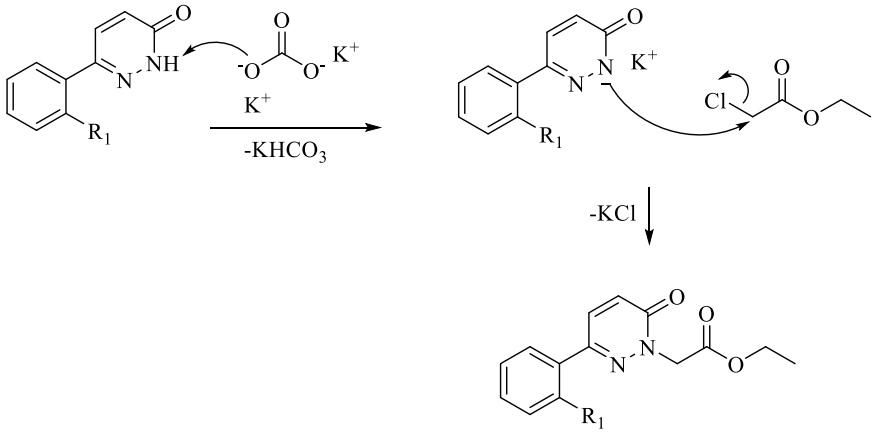

Figure 5. Reaction mechanism for the formation of compound 6

Figure 6. Compound product 6

Synthesis of compound 6

Compound 6 was successfully synthesised through a substitution reaction between pyridazinone and ethyl chloroacetate using K_2CO_3 catalyst in DMF solvent at room temperature. The reaction mechanism for the formation of compound 6 is shown in Figure 5. This synthesis process uses a stirring method, where DMF functions as a solvent with minimal water content, maintaining the effectiveness of the moisture-sensitive reaction, while K_2CO_3 acts as a basic catalyst that accelerates the substitution reaction.

This process produces a yellow solid with a high yield (96.8%) and a melting point of 98°C (Figure 6).

UV analysis shows λmax at 249 nm, reflecting π–π interactions in the aromatic system. The FTIR spectrum shows characteristic bands at 1739 cm^{-1} (C=O ester), 1673 cm^{-1} (C=O), 1592 cm^{-1} (C=N), and 1222 cm^{-1} (C–N), confirming the formation of a pyridazinone structure with an ester group from the substitution reaction.

Compound 8

Compound 8 was synthesised from compound 6 through a hydrazinolysis reaction with phenyl hydrazine in methanol solvent at 80°C [15]. The reaction mechanism can be seen in Figure 7.

After 3 hours of reaction, a yellow solid (Figure 8) was obtained with a yield of 85.8% and a melting point of ±200°C.

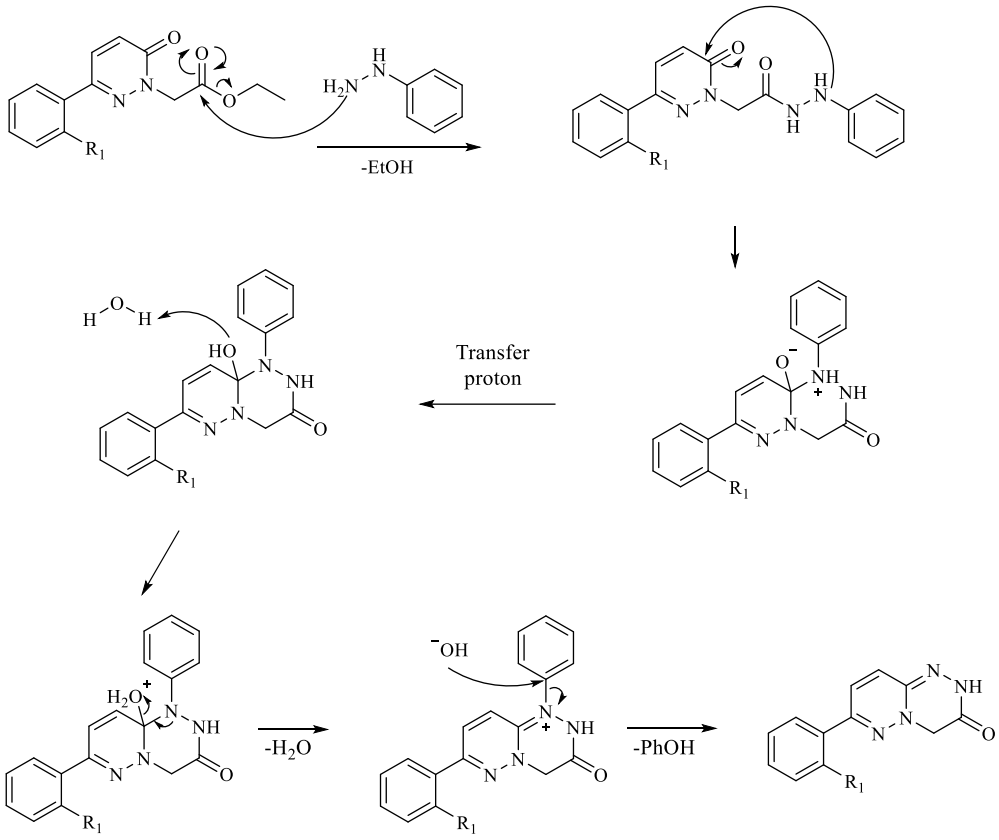

Figure 7. Reaction mechanism for the formation of compound 8

Figure 8. Compound product 8

DOI: https://doi.org/10.25077/jrk.v16i2.809

The UV spectrum shows λmax at 249 nm, indicating the presence of a conjugated aromatic system. FTIR analysis shows characteristic bands for N–H (3500 cm^{-1}), aromatic C–H (3056 cm^{-1}), aliphatic C–H (2937 cm^{-1}), C=O (1667 cm^{-1}), and C=N (1650 cm^{-1}), supporting the formation of a triazinone structure. ^{1}H-NMR data show aromatic peaks in the range of δ 6.9–7.8 ppm, as well as methoxy group peaks at δ 3.88 ppm and methylene (-CH_2-) group peaks at δ 4.79 ppm.

The ^{1}H-NMR analysis of compound 8 is summarised in Table 1, showing several peaks indicating the position of protons on the aromatic ring and the more complex pyridazine structure. The peak at δ 7.85 ppm (doublet of doublets, dd, J = 1.6 Hz, 1H, H-3') indicates the presence of a proton at the 3' position of the phenyl ring bound to the methoxy group. The peak at δ 7.61 ppm (doublet, d, J = 7.6 Hz, 1H, H-5) indicates a proton bonded to the 5th position of the phenyl ring. Additionally, the peak at δ 7.44 ppm (triplet, t, J = 7.3 Hz, 1H, H-5') indicates a proton at the 5' position of the phenyl ring, located near the methoxy group. The peaks at δ 7.12 ppm (dd, J = 1.8 Hz, 1H, H-4) and δ 7.05 ppm (triplet, t, J = 7.7 Hz, 1H, H-4') indicate protons at positions 4 and 4' of the phenyl ring. The peak at δ 6.95 ppm (dd, J = 1.65 Hz, 1H, H-6') indicates a proton at the 6' position on the phenyl ring. The proton on the methoxy group is detected at δ 3.88 ppm (doublet, J = 1.1 Hz, 3H, -OCH_3). The peak at δ 4.79 ppm (singlet, s, 2H, H-1'') indicates a proton at the aliphatic position around the pyridazine structure.

^{13}C-NMR analysis of compound 8, peaks at δ 54.7 ppm (-CH_3) and δ 55.8 ppm (-CH_2-) indicate the presence of methoxy (-OCH_3) and methylene (-CH_2-) groups in the structure. The peak at δ 124.3 ppm (C=C) indicates the presence of a C=C double bond in the phenyl ring, while the peak at δ 172.9 ppm (C=O) indicates the presence of a carbonyl group. The peaks at δ 157.1 ppm and 160.9 ppm (C=N) indicate the presence of an imidazolidine group in the pyridazine ring.

Table 1. Interpretation of 1H-NMR and 13C-NMR data for compound 8

Compound	Position	δ_H	δ_C
8	C=O	-	172,9
	1	-	124,3
	2	-	145,3
	3	7,85 (dd, *J* = 1.6 Hz, 1H)	127,3
	4	7,05 (t, *J* = 7,7 Hz, 1H)	111,2
	5	7,44 (t, *J* = 7,3 Hz, 1H)	130,0
	6	6,95 (dd, *J* = 1,65 Hz, 1H)	120,6
	7	-	157,2
	8	7,12 (d, *J* = 8,45 Hz, 1H)	135,1
	9	7,61 (d, *J* = 7,6 Hz, 1H)	130,7
	10	-	160,9
	-CH_2-	4,79 (s, 2H)	55,8
	-OCH_3	3,88 (s, 3H)	54,7

Table 2. Bond energy and bond type results of molecular docking of compound 8 against 1T46

Compound	S (kkal/mol)	RMSD	Hydrogen Bond	Other interactions
Natural ligan	-6.5142	1.3101	Cys637, Asp810,Thr670, Glu640	Phe811, Leu799, Leu644, Leu595, Tyr672, Val603, Ala621, Lys623, Val654, Val643
Doxorubicin	-10.1415	1.3389	Ile789, Arg791, Asp810	Val643, His790, Glu640, Leu644, Leu813, Ala636
compound 8	-9.1971	0.9092	Cys673	Leu799, Ala621, Leu595, Val603, Cys809, Phe811

Molecular Docking

The bioactivity of synthesised compounds in inhibiting protein kinase was analysed using the molecular docking method. This method aims to perform virtual screening, predict poses, and estimate binding affinities [16]. Molecular docking is an effective method for predicting and identifying desired bindings, determining the possible conformations of a compound, and analysing the interactions between ligands and receptors [17].

Molecular docking of compound 8 was performed using MOE 2022.02 software against the α-estrogen receptor (PDB ID 1T46), which was used as a target for breast cancer treatment. The native ligand was used as a control to validate the docking results. The docking results showed that compound 8 has good affinity for the 1T46 receptor, as reflected by the low bond free energy and the types of interactions formed. The docking results are presented in Table 2, which shows various interactions between the compound and the amino acid residues present at the active site of the receptor.

The bond free energy of compound 18a is -9.1971 kcal/mol, while compound 18b has a slightly lower bond free energy value of -9.7904 kcal/mol. The more negative the bond free energy value, the stronger the interaction between the ligand and the receptor, indicating the potential of this compound to bind well to the 1T46 receptor. The RMSD (Root Mean Square Deviation) of compound 8 is 0.9092 Å, indicating that the docking results are sufficiently stable and valid, given that the RMSD value is less than 2 Å. The docking process can be considered valid if the RMSD value is less than 2 [17]. This indicates that the ligand conformation generated by the software is sufficiently close to the natural or control ligand position, demonstrating the accuracy of the docking method used.

The main interactions found in the docking results of compound 8 with the 1T46 receptor are hydrogen bonds and hydrophobic interactions (Figure 9). Compound 8 interacts with amino acid residues such as Cys673, Thr670, and Asp810 through hydrogen bonds. These interactions contribute to the stability and binding affinity between the compound and the receptor. Additionally, the hydrophobic interactions formed between the compound and residues such as Leu595, Cys809, and Lys623 indicate the compound's potential to bind to the hydrophobic sites on the receptor, which could enhance affinity and selectivity toward the target.

Comparison with natural ligands shows that compound 8 has better or equivalent potential in forming bonds with the active site of the receptor. The natural ligand (PDB ID 1T46) has a bond free energy of -6.5142 kcal/mol, involving hydrogen bonds with residues such as Cys637, Asp810, Thr670, and Glu640, as well as various hydrophobic interactions. In this case, compound 8 exhibits a lower binding free energy value, indicating that compound 8 has a higher potential to bind to the receptor compared to the natural ligand.

 DOI: https://doi.org/10.25077/jrk.v16i2.809

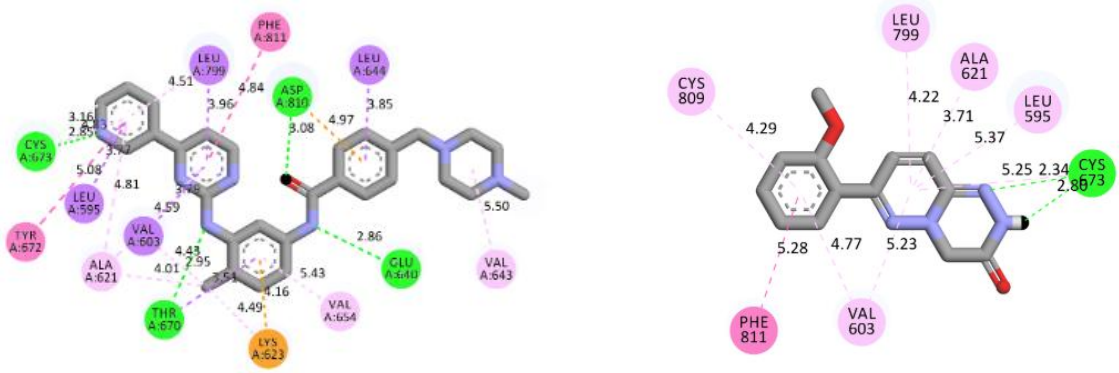

(a) **(b)**

Figure 9. Visualisation of docking results (a) Doxorubicin, (b) Compound 8

Conclusions

This study successfully synthesised methoxy- and phenyl-substituted pyridazinone derivatives and phenyl hydrazine through a multi-step pathway, starting from 2-methoxyacetophenone and glyoxylic acid to produce the target compound 7-(2-methoxyphenyl)-2H-pyridazino[6,1-c] [1,2,4]triazine-3(4H)-one (compound 8). The synthesis results demonstrated high yields and confirmed structures through spectroscopic analysis (UV-Vis, FTIR, NMR, MS) and chromatography (TLC, HPLC). In silico testing with molecular docking against the α-estrogen receptor (PDB ID: 1T46), which plays a crucial role in breast cancer, showed that compound 8 has a strong binding affinity with a free energy of –9.1971 kcal/mol and stable interactions with residues Cys673, Leu799, and Phe811. This value is superior to natural ligands and approaches the activity of doxorubicin as a reference drug. These results confirm that structural modifications of pyridazinone with methoxy and phenyl hydrazine substituents enhance cytotoxic activity and have potential as new, more selective anticancer drug candidates with a lower toxicity profile compared to conventional therapies.

Acknowledgements

We would like to express our gratitude to the Research and Community Service Institute, University of Riau and Directorate General of Research, Technology and Community Service, KEMDIKBUDRISTEK, Republic of Indonesia, which has provided funding and facilities for this research with contract numbers 20741/UN19.5.1.3/AL.04/2024 and 19536/UN19.5.1.3/AL.04/2025.

References

1. Singh, J., Kumar, V., Silakari, P., Kumar, S. 2023. Pyridazinones: A versatile scaffold in the development of potential target-based novel anticancer agents. *In Journal of Heterocyclic* Chemistry. 60 : 6.
2. Merde, İ.B., Önel, G.T., Akkoç, S., Karaköy, Z., Türkmenoğlu, B. 2023. Focusing on new piperazinyl-methyl-3(2H)pyridazinone based derivatives: Design, synthesis, Anticancer activity and Computational studies. *ChemistrySelect*. 8(25). https://doi.org/10.1002/slct.202300910.
3. Asif, M. 2019. A review on pyridazinone ring containing various cardioactive agents. *Journal of chemical*.
4. Partap, S., Akhtar, M.J., Yar, M.S., Hassan, M.Z., Siddiqui, A.A. 2018. Pyridazinone hybrids: design, synthesis and evaluation as potential anticonvulsant agents. *Bioorganic Chemistry*. 77: 74–83.
5. Tiryaki, D., Sukuroglu, M., Dogruer, D.S., Akkol, E., Sahin, M.F. 2013. Synthesis of some new 2,6-disubstituted-3(2H)-pyridazinone derivatives and investigation of their analgesic, anti-inflammatory and antimicrobial activities. *Medicinal Chemistry Research*. 22 (6): 2553–2560.
6. Siddiqui, A.A., Mishra, R., Shaharyar, M. 2010. Synthesis, characterization and antihypertensive activity of pyridazinone derivatives. *European Journal of Medicinal Chemistry*. 45 (6): 2283–

2290.

7. Ritchie, T.J., Macdonald, S.J., Peace, S. 2012. The developability of heteroaromatic and heteroaliphatic rings–do some have a better pedigree as potential drug. *Med Chem Comm*. 3 : 1062–9.
8. Jaballah, M.Y., Serya, R.T., & Abouzid, K. 2017. Pyridazine based scaffolds as privileged structures in anti-cancer therapy. *Drug Res (Stuttg)*, 67(3): 138–48.
9. Merde, İ.B., Önel, G.T., Akkoç, S., Karaköy, Z., & Türkmenoğlu, B. 2023. Focusing on new piperazinyl-methyl-3(2H)pyridazinone based derivatives: Design, synthesis, Anticancer activity and Computational studies. *ChemistrySelect*, 8(25): e202300910.
10. Merde, İ.B., Önel, G.T., Akkoç, S., Karaköy, Z., & Türkmenoğlu, B. 2023. Focusing on new piperazinyl-methyl-3(2H)pyridazinone based derivatives: Design, synthesis, Anticancer activity and Computational studies. *ChemistrySelect*, 8(25): e202300910.
11. Blume-Jensen, P., & Hunter, T. (2001). *Oncogenic kinase signalling*. Nature, 411, 355–365.
12. Wu, X., *et al*. (2020). *Design, synthesis and biological evaluation of pyrazolo[3,4-d]pyridazinone derivatives as covalent FGFR inhibitors*. Acta Pharmaceutica Sinica **B**, 11(3), 781–794.
13. Ali, S., Rasool, M., Chaoudhry, H., Pushparaj, P. N., Jha, P., Hafiz, A., & Jamal, M.S. 2016. Molecular mechanisms and mode of tamoxifen resistance in breast cancer. *Bioinformation*, 12(3): 135–139.
14. Chung, C. (2017). "Pyridazinone Synthesis and Reaction Mechanisms." *Journal of Medicinal Chemistry*, *60*(1): 23–38.
15. Özdemir, A., Demirci, F., Abu Mohsen, U., & Kaplancıklı, Z. A. (2013). *Synthesis and antifungal activity of new hydrazide derivatives*. Journal of Enzyme Inhibition and Medicinal Chemistry**,** 28(6), 1211–1216.
16. Adelusi, T. I., Oyedele, A. K., Boyenle, I. D., Ogunlana, A. T., Adeyemi, R. O., Ukachi, C. D., Idris, M. O., Olaoba, O. T., Adedotun, I. O., Kolawole, O. E., Xiaoxing, Y., Abdul-Hammed, M. (2022). *Molecular modeling in drug discovery***.** Informatics in Medicine Unlocked**,** 29, 100880.
17. N. Frimayanti, M. Yaeghoobi, H. Namavar, M. C. Utari, M. Djohari, and C. O. Laia, "In silico analysis approach for screening new agents for breast cancer inhibitors based on 1,5-benzothiazepine," *Pharm. Sci. Asia*, vol. 49, no. 5, 2022, doi: 10.29090/psa.2022.05.22.001.

 DOI: https://doi.org/10.25077/jrk.v16i2.809